Aalborg Universitet

Mobile Handset Performance Evaluation Using Radiation Pattern Measurements

Nielsen, Jesper Ødum; Pedersen, Gert Frølund

Mobile Handset Performance Evaluation Using Radiation Pattern Measurements

Jesper Ødum Nielsen and Gert Frølund Pedersen

Abstract—The mean effective gain is an attractive performance measure of mobile handsets, since it incorporates both directional and polarization properties of the handset and environment. In this work the mean effective gain is computed from measured spherical radiation patterns of five different mobile handsets, both in free space and including a human head & shoulder phantom. Different models of the environment allow a comparison of the mean effective gain obtained for realistic models based on measurements with the total radiated power and the total isotropic sensitivity. All the comparisons are based on the mean effective gain values obtained for different orientations of the handsets in the environments. For practical measurements it is important to minimize the measurement time. The paper includes a study of the variation in mean effective gain when the number of samples in the spherical radiation pattern is reduced. Furthermore, the frequency dependence of the mean effective gain is investigated, and a method is proposed for reducing the required number of measurements on different frequencies.

Index Terms—Frequency dependence, mean effective gain (MEG), mobile handset performance, sampling density, spherical radiation pattern, total isotropic sensitivity (TIS), total radiated power (TRP).

I. INTRODUCTION

ONE IMPORTANT aspect of a mobile handset is its ability to receive and transmit signal power. The performance in this respect is important for both the user and the network operator, since the battery lifetime of a handset will be influenced, as will the network coverage and capacity.

The received signal power depends directly on the transmitted power level in addition to the orientation and polarization properties at the transmitter and the receiver, as described by the antenna radiation patterns. Inclusion of the directional and polarization properties of the transmitted or received power is difficult for mobile handsets, since the handsets often are used in a multipath environment, where the signal may be received from many directions and with different polarizations [1]. One way to characterize the performance of a mobile handset in a realistic way is to use the so-called mean effective gain (MEG). Using a known antenna as reference, the MEG measures the mean received power in a realistic mobile environment [2]. The MEG is an attractive measure since it incorporates both directional and polarization properties of the mobile channel and the handset.

A straightforward way to obtain the MEG for a handset is to measure the antenna output signal using a cable connection to some equipment such as a channel sounder or a power meter.

With this method it is relatively easy to include live persons in the measurements and study the influence of the human operator on the handset performance [3], [4]. Adding conductive cables to a handset may be a problem, since this will change the radiation properties of the handset. An efficient way to avoid these problems is to implement an optical link between the handset and any measurement equipment [5].

Another possible way to avoid the cables is to utilize the measurement capabilities built-in, e.g., the GSM network. During normal calls the network is regularly performing signal strength measurements to aid the hand-over process, and by dedicated equipment this data can be collected from the network [6], [7]. Obviously, this method is limited to measurements with already functional handsets, but on the other hand it can be very realistic.

Performing measurements in the mobile environment has some disadvantages, such as the setup of the necessary equipment and the planning. Furthermore, transmitting on the relevant frequencies may require a licence. Instead attempts have been made to simulate the multipath propagation environments in so-called scattered field measurements, where a room is designed to create a multipath environment for a handset, see section 3.5.2.2 of [8]. Similar artificial propagation environments are created in the so-called stirred mode chamber [9], [10] which is a shielded chamber with metal walls and a number of moving metallic parts which change the field inside the chamber. The main problem of these methods using artificial environments is in controlling the signal distribution inside the room and that the created mobile environment is not necessarily typical for a mobile in real use [11].

Alternatively, it is possible to separate measurements of the antenna and the environment. Using the spherical radiation pattern of the antenna and a model of the power distribution in the environment versus direction, the MEG may be computed using a surface integral [1], [12]. This method of testing is quite flexible since the radiation patterns of handset antennas can be simulated using models of the handset and its user [13]–[15]. Existing handset products or prototypes can be measured in an anechoic room including users [16], [17]. Also, this method allows testing in different environments using the same radiation pattern measurement or simulation [18], [19].

In practice the surface integral involved in obtaining the MEG has to be computed from a finite set of samples of the spherical radiation pattern. Since the individual measurements are time consuming there is a tradeoff between the accuracy and the time it takes to collect the measurements. Furthermore, if the radiation patterns are obtained from battery powered handsets, there is a limit on the acceptable total measurement time. In addition, the radiation patterns are generally frequency dependent and hence they may have to be measured at multiple fre-

quencies. Therefore, some investigations are required as to how densely the radiation patterns need to be sampled for a given accuracy, and on how many frequencies. These investigations may be based on measurements, since investigations of each contributor to the error such as reflections, measurement errors, position errors, calibration errors, etc., are a much larger task.

In this work the MEG is computed using spherical measurements of the radiation patterns of four commercially available mobile handsets, one of which is measured with two different antennas. Five different models of the mobile environment are used and it is investigated how the accuracy of the MEG calculations depend on the sampling density of the spherical radiation patterns. The frequency dependence of the MEG is investigated using measurements carried out on different frequencies, both in free space and using a phantom of the human body.

II. MEAN EFFECTIVE GAIN

As detailed in [1], [12], the MEG may be obtained using a surface integration

$$\Gamma(f) = \frac{\oint_S G_\theta(\Omega, f) Q_\theta(\Omega, f) + G_\phi(\Omega, f) Q_\phi(\Omega, f) d\Omega}{\oint_S Q_\theta(\Omega, f) + Q_\phi(\Omega, f) d\Omega}. \quad (1)$$

Using ψ to denote either θ or ϕ, $G_\psi(\Omega, f)$ is the antenna power gain in the ψ-polarization versus direction Ω and at the frequency f, computed as the measured power normalized to the total input power. The interpretation of $Q_\psi(\Omega, f)$ depends on the link direction. For the down-link (DL), $Q_\psi(\Omega, f)$ is the average power incident on the handset from the direction Ω in the ψ-polarization. For the up-link (UL), $Q_\psi(\Omega, f)$ is the power received on average by the base station stemming from the mobile transmitting in the direction Ω and in the ψ-polarization. In this work $Q_\psi(\Omega, f)$ is assumed to be frequency independent within the band of interest and the frequency variable f is omitted henceforth.

In this work five models of the power densities $Q_\theta(\Omega)$ and $Q_\phi(\Omega)$ have been used. Since MEG is a ratio of power values only the cross polarization difference (XPD) and the distribution of power versus direction is important. The models are described as follows.

AAU: A model based on numerous outdoor to indoor measurements in the city of Aalborg, Denmark [20]. This model is non-uniform versus both azimuth and elevation angle, and has an XPD of 5.5 dB.

HUT: A model based on numerous outdoor to indoor measurements in the city of Helsinki, Finland [19]. In this model the variation versus azimuth angle is assumed uniform and non-uniform versus elevation angle. It has an XPD of 10.7 dB.

Rect0: The rectangular model proposed in [21] has uniform weighting inside the window defined by $45° \leq \theta \leq 135°$ for all ϕ, and zero weighting outside this window, where θ is the elevation angle measured from the vertical axis and ϕ is the azimuth angle. The XPD is 0 dB for this model.

Rect6: Similar to Rect0, but with an XPD of 6 dB.

Iso: The hypothetical isotropic model implies equal weighting of power versus direction in both polarizations and with an XPD of 0 dB. This model results in MEG values

equivalent to the total radiated power (TRP) and total isotropic sensitivity (TIS), for the UL and DL, respectively.

The TRP and TIS have been suggested as initial handset antenna performance measures for the UL and DL, respectively, but the TRP/TIS does not include the directional and polarization aspects, and hence may be misleading. It should be noted that the MEG values obtained with the isotropic environment differ from the true TRP/TIS since they are based on the antenna gain patterns. The TRP is defined as

$$P_{\text{TRP}} = \frac{P_{\text{Tx}}}{4\pi} \oint_S G_\theta(\Omega) + G_\phi(\Omega) d\Omega = 2P_{\text{Tx}} \Gamma_{\text{Iso}}$$

where P_{Tx} is the nominal (or conducted) transmit power level of the handset and Γ_{Iso} is the MEG value obtained with the isotropic model. Hence, the TRP can be found from the MEG value via a simple scaling. Likewise, the TIS is $P_{\text{TIS}} = P_{\text{c}}/(2\Gamma_{\text{Iso}})$ where the conducted power (at the receiver input) resulting in the receiver operating with a bit error rate of 2.44% is defined to be $P_{\text{c}} = -102$ dBm. In this work the differences in Γ_{Iso} and TRP/TIS values are ignored.

The Rect0 model was proposed by the Cellular Telecommunications & Internet Association (CTIA) in [21] as a "Near-Horizon Partial Isotropic Sensitivity" and may be viewed as a very simple model of the power distribution in the environment. Although this model does not appear to be accurate in many cases, it does incorporate that in many mobile environments the power is not likely to arrive, e.g., from directly above the handset. On the other hand, dense urban environments with high rise buildings may result in power coming from reflections or refractions high above the handset user [12]. The Rect6 model is a simple attempt to add some typical polarization aspects into the Rect0 model.

III. MEASUREMENTS AND DATA PROCESSING

The measurements used in this work were performed in a large anechoic room using a GSM tester (Rohde & Schwarz CMU 200) and a positioning device with two axes, see Fig. 1. Both the CMU tester and the positioning device are controlled by locally developed software running on a SUN workstation, allowing automatic measurement of the complete spherical radiation pattern in both the θ- and the ϕ-polarization. The CMU tester, acting as a base station, measures the UL power while the DL measurements are obtained from the power levels measured by the handset, as required by the GSM standard. In this way the measurements can be made without any modifications of the handsets, such as attaching cables, etc., which will change the radiation pattern [5].

The power measurements carried out by the handsets are intended for power control and handover decisions and hence are not precision measurements. According to the GSM standard the reported power levels are allowed to deviate up to 6 dB from the actual power level [22]. Therefore, a calibration procedure must be applied before the data can be used for the DL. This is possible using the reported power levels for a sweep of known input power levels in addition to a single measurement of the power levels necessary for the receiver to operate at the sensitivity level defined at the 2.44% bit error rate. In practice deviations are small for the handsets used in this campaign. The de-
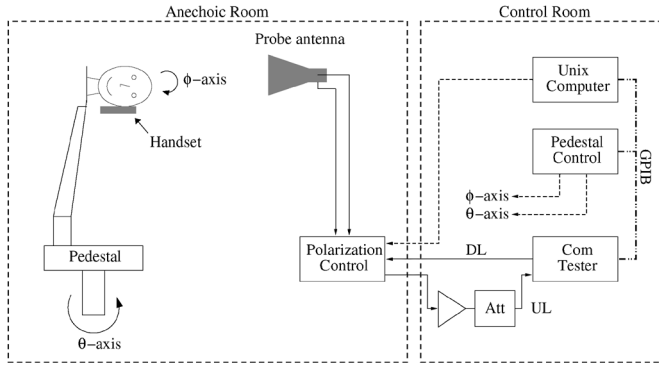
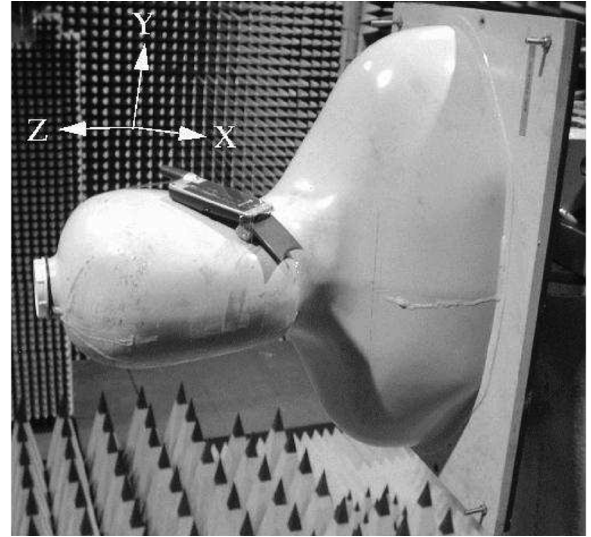Fig. 1.   Block diagram of the radiation pattern measurement system.

Fig. 2.   A handset mounted on the phantom.

Fig. 3.   Measured power gain pattern for handset C including the phantom and measured on the center channel in the DL.

viations from linearity versus input power of the measurements made by the handsets were determined via measurements to be less than about 0.7 dB within a dynamic range of 30–35 dB from the maximum received power. Hence, the relative errors are of the same order as the quantization error due to the 1 dB steps. In addition there may be a constant offset in the absolute values reported by the handsets. This offset could be determined but was not done in the current work.

Spherical radiation patterns of four commercially available GSM handsets have been measured. Handset A and B are large handsets with external and internal antennas, respectively. Handset C and F are small handsets with internal and external antennas, respectively. Here "small" handsets are about 10 cm by 4.5 cm, and the "large" handsets are about 13 cm by 4.5 cm. Handset F was also measured with a substitute antenna (a retractable dipole); these measurements are labeled handset E.

All the handsets were measured on the GSM-1800 channels 512, 698, and 885, corresponding to about 1805, 1842, and 1880 MHz for the DL, respectively, and about 1710, 1747, and 1785 MHz for the UL. These channels are the center and two edge channels of the GSM-1800 frequency band. The spherical radiation patterns were sampled using increments of $10°$ in both the azimuth angle ϕ and the elevation angle θ (see also Section V). As usual, the elevation angle is defined as the angle between the point and the z-axis, and the azimuth angle between the x-axis and the projection of the point on the xy-plane. The handsets were measured both in free space and next to a phantom head (Schmid & Partners v. 3.6), which was filled with a tissue simulating liquid [23]. For the free space measurements the handsets were oriented along the z-axis of the coordinate system with the display pointing towards the negative y-axis. When the phantom was included, the handset was mounted on the left side of the phantom head at an angle of $45°$ from the z-axis, still with the display side facing the negative y-axis, see Fig. 2. An example of a measured power gain pattern is shown in Fig. 3.

For real handsets in actual use both the radiation pattern and the spherical power distribution are directional and the MEG will vary depending on the orientation of the handset with respect to the environment. Therefore, it is necessary to consider more than one MEG value and, e.g., compute a mean value. In addition, the variation in MEG for an environment is of interest; for example the MEG might be unacceptably low in some cases although the mean is acceptable.
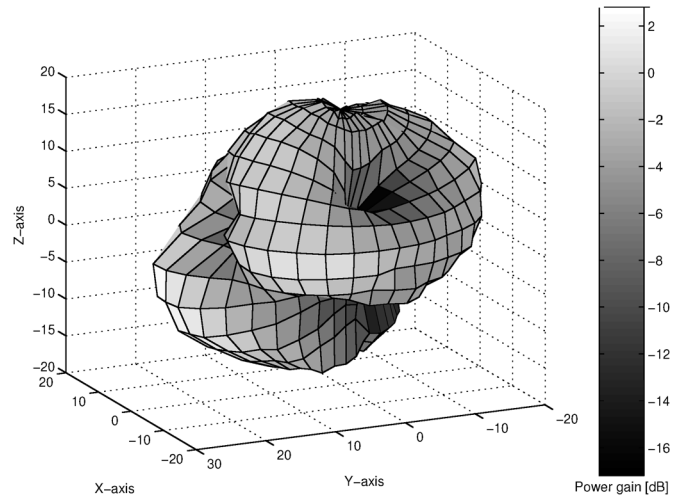
In order to investigate the variation in MEG, the measured radiation patterns have been rotated firstly with an angle of λ about the y-axis, corresponding to the phantom either bending forward or backward, and afterwards with an angle μ about the z-axis, corresponding to the phantom turning around in azimuth. For each desired point of the rotated pattern the coordinates for the corresponding point in the actually measured pattern is found and the measured θ- and ϕ-polarization components are mapped according to the rotation and coordinates. As samples are needed from directions not in the original sampling grid, spline interpolation has been used to obtain the rotated radiation patterns. All combinations of $\mu \in \{0°, 15°, 30°, \ldots, 345°\}$ and $\lambda \in \{0°, 15°, \ldots, 60°, 300°, 315°, \ldots, 345°\}$ have been used and for each combination of λ and μ the MEG was computed. Note that for the phantom measurements the described post processing rotation procedure corresponds to a simultaneous rotation of both the handset and the phantom.

The repeatability of the measurements has been investigated in order to determine the level of uncertainty in the MEG computations. For two different handsets (handset A and C) the max-

Fig. 4. MEG for free space conditions for both the UL (top) and the DL (bottom). The vertical line endpoints indicate minimum and maximum values.
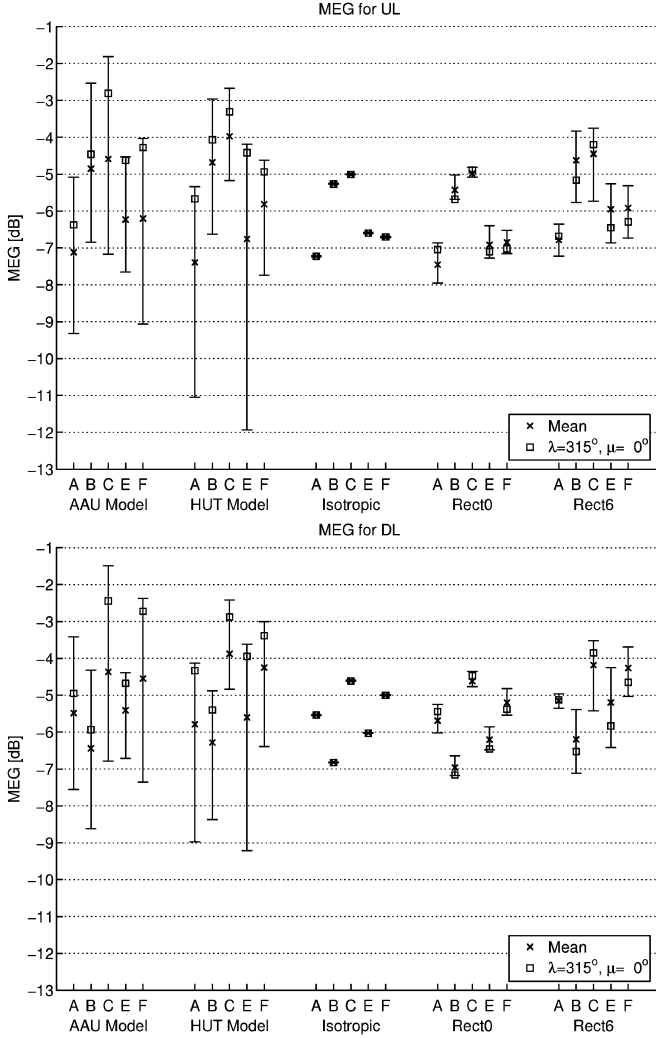

Fig. 5. MEG for handset including phantom for both the UL (top) and the DL (bottom). The vertical line endpoints indicate minimum and maximum values.

imum difference in the MEG computed from nine repeated free space measurements was 0.2–0.4 dB, depending on the handset, link direction and environment model. The values were computed as an average for the different orientations of the handsets. For three repeated measurements including the phantom the maximum difference was found to be 0.1–0.3 dB.

The accuracy of the measured values has been verified by the work in [24] where measurements made in the anechoic room on a monopole and a patch antenna were compared to finite difference time domain (FDTD) simulations of the same antennas. A good agreement was found between the simulated and measured radiation patterns both having the same overall shape. The absolute value in each direction and polarization was usually within a few dB's. This is acceptable because the deviations are averaged in the MEG computation and because the largest deviations are where the absolute power level is low.

IV. MEG FOR DIFFERENT ENVIRONMENTS

Fig. 4 shows the MEG values obtained with the handsets in combination with different models of the environment, for the free space case, and for both the UL and DL. The corresponding

results for the phantom measurements are given in Fig. 5. The MEG values as given by (1) are approximated using the formula

$$\Gamma_{p,q}(\lambda,\mu) \simeq \sum_{n=0}^{\frac{N-1}{p}} \sum_{m=0}^{\frac{M}{q}-1} [G_\theta(\theta_{p\cdot n},\phi_{q\cdot m};\lambda,\mu)Q_\theta(\theta_{p\cdot n},\phi_{q\cdot m})$$
$$+ G_\phi(\theta_{p\cdot n},\phi_{q\cdot m};\lambda,\mu)Q_\phi(\theta_{p\cdot n},\phi_{q\cdot m})]\frac{\sin(\theta_{p\cdot n})}{P_{\text{env}}} \quad (2)$$

where

$$P_{\text{env}} = \sum_{n=0}^{\frac{N-1}{p}} \sum_{m=0}^{\frac{M}{q}-1} [Q_\theta(\theta_{p\cdot n},\phi_{q\cdot m}) + Q_\phi(\theta_{p\cdot n},\phi_{q\cdot m})]\sin(\theta_{p\cdot n})$$

and $G_\psi(\theta_n,\phi_m;\lambda,\mu)$ is the antenna power gain for the ψ-polarization in the direction given by (θ_n,ϕ_m) and for a rotation of the antenna using the angle pair (λ,μ). In the following Section V decimation of the measured radiation patterns are studied by using different values of p and q, but the results presented in this section were computed without decimation and hence $p = q = 1$ in (2). Furthermore, all results presented in this

TABLE I
XPD IN dB FOR THE MEASURED RADIATION PATTERNS. NOTE THAT ROTATION
OF THE PATTERNS CHANGE THE XPD

Handset	Free Space		Phantom	
	DL	UL	DL	UL
A	3.7	5.2	0.3	1.3
B	8.2	8.7	−2.6	−2.5
C	3.8	4.4	−5.0	−3.8
E	13.7	11.8	−1.6	−2.4
F	8.9	9.2	−5.9	−5.6

section are based on measurements made at the center of the GSM-1800 band, channel 698.

As mentioned above, the MEG is computed for many different orientations of the handsets in order to evaluate both a mean MEG and to estimate the variation in the MEG as function of orientation. In the figures the minimum and maximum of the computed MEG values are shown as the endpoints of a vertical line, one line for each handset. Also shown on each line is the mean value (shown with "×") and a MEG value for a specific orientation, marked with "□" (see later). The results are presented in groups, one for each of the environments defined in Section II.

Comparing the TRP and TIS results with those obtained using the rectangular window model (XPD of 0 dB) it is noticed that the results are very similar. The mean values are roughly identical, which is expected since the rectangular window covers about 71% of the sphere surface area. Hence, most of the power will be included, and as the XPD is zero no polarization weighting is used. Therefore the results will essentially be the TRP/TIS results.

Because the measured radiation pattern is rotated up to 60° in elevation angle some variation in the MEG values are observed for the rectangular window model, but only small changes are noticed compared to the changes seen with the two environment models derived from measurements. The rectangular window model with an XPD of 6 dB causes more changes, but the results are still far from those obtained with the AAU and HUT models.

Although the results obtained with the AAU model and the HUT model have some similarities, it is also clear that there are significant differences in some cases. For example for handset E in the free space case the two models result in a MEG variation of about 2.4 and 5.5 dB for the AAU and HUT model in the DL direction, respectively, and about 3.1 and 7.7 dB for the UL direction.

The large difference for the two models illustrates that both the power distribution versus angle and the XPD is important. The fact that before rotation handset E has a null near $\theta = 90°$, where the HUT model has most of the power concentrated, combined with a high XPD of both handset E in free space and the HUT model yields MEG values which are highly dependent on the orientation. Table I shows the XPD for all the measurements, where it is noticed that the XPD may differ for the DL and UL. Hence, the frequency difference between the DL and UL must play a role.

Comparing Fig. 4 and Fig. 5 is seems that the measurements including the phantom generally have a larger difference between the minimum and the maximum MEG, than the corresponding free space measurements. This is due to the phantom which blocks some of the power and effectively makes the radiation patterns more directive than the free space patterns. This causes more changes in the MEG when the handset is rotated and the environment model is directive as well.

Table II shows the differences in the mean MEG values obtained with the various environment models compared to the TRP/TIS (i.e., isotropic environment). The table is for the measurements including a phantom. A similar table for the free space shows that all differences are within the range −0.3 up to 1.0 dB.

The mean values are also quite small with the phantom in case of the rectangular window model with an XPD of 0 dB, where all differences are smaller than or equal to 0.4 dB. However, for the other models larger differences are found. In particular the HUT model results in differences from −1.9 up to 0.8 dB.

It is important to realize that even if the mean values are identical for two different models of the environment, this does not imply that the MEG values obtained with the two models are identical for a specific rotation of the radiation pattern. For the free space an example is the rotation of the measured radiation pattern with $\lambda = 315°$ and $\mu = 0°$, corresponding to a tilt angle of 45° in typical talk position. The MEG values obtained with these rotations are shown on the vertical lines in Fig. 4 with a "□." It is clearly not possible to predict the MEG values shown with the □-marks from the mean values. The same is also true for the phantom measurements (Fig. 5). For the phantom measurements $\lambda = 0°$ and $\mu = 0°$ is used since the handset is already mounted at an angle of 45° on the phantom. The MEG values obtained with the different models are depicted in Fig. 6, where the MEG is shown sorted for increasing TRP. Each line in the plot represents a model of the environment and the values are all obtained with the same orientation of the handset/phantom as used above.

The MEG for the AAU, HUT, and Rect6 models are not monotonically increasing, showing that the MEG values for these models cannot be predicted from the TRP values. As expected, the results for the Rect0 model are roughly similar to the TRP values, except for a constant offset.

V. SPHERICAL SAMPLING DENSITY

In [25] it was shown that the field originating from a collection of scatterers is approximately band limited, so that the field pattern can be reconstructed from samples on a sphere if the angular sampling interval in both elevation and azimuth is smaller than $2\pi/(2M+1)$, with $M = \text{Int}(\chi ak) + 1$. In this expression $\text{Int}(\cdot)$ denotes the integer part of the enclosed value, a is the radius of the smallest possible sphere circumscribing the collection of scatterers, $k = 2\pi/\lambda$ is the wave-number, and χ is an excess bandwidth factor allowing control of the approximation error. The formula assumes fixed angular increments.

For the phantom measurements the radius of the combined handset and phantom is of the order $a = 0.25$ m and if the frequency is 1880 MHz, then $M = 15$ if $\chi = 1.44$ as suggested in [25]. This corresponds to a minimum sampling density of about 11.6° if complex samples are obtained. When power values are measured the sampling interval needs to be halved [26]. It should be noted that the above criterion ensures reconstruction of the radiation pattern whereas the intended applica-

TABLE II
DIFFERENCE IN MEAN MEG VALUES WITH THE ISOTROPIC CASE AS REFERENCE. ALL VALUES ARE IN dB AND FOR THE PHANTOM CASE

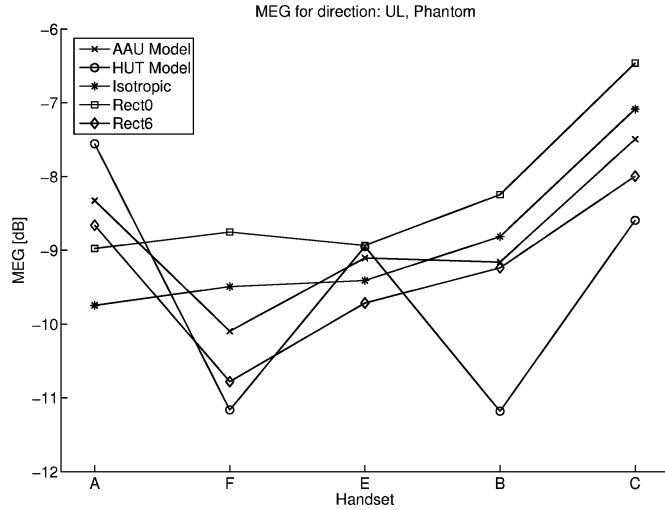| Environment	Handset, DL					Handset, UL				
	A	B	C	E	F	A	B	C	E	F
AAU	0.1	−0.7	−1.1	0.1	−0.9	0.2	−0.8	−1.0	−0.1	−0.9
HUT	0.8	−1.0	−1.9	0.0	−1.6	0.8	−1.2	−1.6	−0.3	−1.5
Isotropic	0.0	0.0	0.0	0.0	0.0	0.0	0.0	0.0	0.0	0.0
Rect0	0.3	0.1	0.3	0.4	0.4	0.3	0.1	0.2	0.3	0.3
Rect6	0.2	−0.6	−1.0	0.4	−0.7	0.3	−0.6	−0.9	0.1	−0.7

Fig. 6. MEG for a specific orientation ($\lambda = 0°$ and $\mu = 0°$) sorted for increasing TRP. All values are for the phantom case.

TABLE III
MEAN MEG ERROR IN dB DUE TO INTERPOLATION USED IN ROTATION OF SIMULATED RADIATION PATTERNS FOR FREE SPACE. THE VALUES ARE AVERAGED OVER THE FIVE SIMULATED HANDSETS

$(\Delta_\theta, \Delta_\phi)$	AAU	HUT	ISO
(5,5)	0.0	0.0	0.0
(10,10)	0.1	0.1	0.1
(20,20)	0.6	0.7	0.5
(30,30)	1.5	1.8	1.3
(60,60)	0.8	1.4	1.0
(10,20)	0.1	0.1	0.1
(10,30)	0.2	0.2	0.2
(10,40)	0.4	0.5	0.4
(10,60)	0.8	0.7	0.7

tion of the measurements in this work is for computing MEG values and hence a less dense sampling may be acceptable.

In order to investigate the necessary sampling density further, some FDTD simulations were carried out, allowing a study without the errors which are inevitable in practical measurements, such as noise and reflections in the anechoic room.

Five antennas were simulated which were similar to the measured handsets, a small and a large handset with either an internal patch antenna or an external helix antenna. Also a small handset with a whip antenna was simulated. The small and large simulated handsets have the same dimensions as the real handsets and were simulated in free space on the frequencies corresponding to the GSM-1800 channels 512, 698, and 885 for both UL and DL. The radiation patterns were simulated with 1° steps in both the θ- and ϕ-angle.

Different decimation factors p and q have been tested for the θ and ϕ angles, respectively, so that the resulting angular sampling intervals are $p\Delta_\theta$ for the elevation angle and $q\Delta_\phi$ for the azimuth angle, where $\Delta_\theta = \Delta_\phi = 1°$. The MEG was computed for different combinations of the decimation factors $p, q \in \{1, 4, 6, 9, 10, 12, 15, 20, 30\}$ and the change in the MEG was investigated using the normalized MEG

$$\Gamma'_{p,q}(\lambda, \mu) = \frac{\Gamma_{p,q}(\lambda, \mu)}{\Gamma_{1,1}(\lambda, \mu)} \quad (3)$$

where $\Gamma_{p,q}(\lambda, \mu)$ is the MEG obtained using (2).

As mentioned above, computation of the radiation pattern for the rotated antenna requires samples that are not in the original sampling grid and therefore interpolation has been used. For the results of the current work which are based on measured radiation patterns, such as in Section IV, the interpolation is based on the decimated measurements, since this is what will happen in practice if only one spherical radiation pattern is measured for each handset. However, for the results discussed in the current section the interpolation of the simulated radiation patterns is based on the original 1° × 1° sampling grid, even when decimation is used. In this way interpolation errors are essentially eliminated and the influence of sampling density can be studied separately. Table III shows the mean error introduced if the decimation is done before the interpolation, i.e., mimicking the situation when the radiation patterns were measured in the specified grids.

For each orientation of the handset a value of $\Gamma'_{p,q}$ is obtained indicating that the error in the MEG may depend on the orientation of the handset. From statistics of the MEG change it was concluded that the error is essentially the same for all the frequencies. Fig. 7 shows the maximum absolute errors for each combination of simulated handset, decimation factor, and environment model. The handsets are labelled $Sa, Sb, \ldots, Se$.

As expected the error is generally lowest for the isotropic environment with negligible errors for sampling in 20° × 20° or 10° × 40° grids, or better. It is noticed that the HUT model generally require a denser sampling than the AAU model which can be explained by the fact that the AAU model is less directive in the elevation angle than the HUT model.

Another interesting observation is that the largest errors usually are obtained for the Sc antenna which is the small handset with external helix antenna, and not the large handset, as might be expected. However, the Sc antenna has a null near $\theta = 90°$
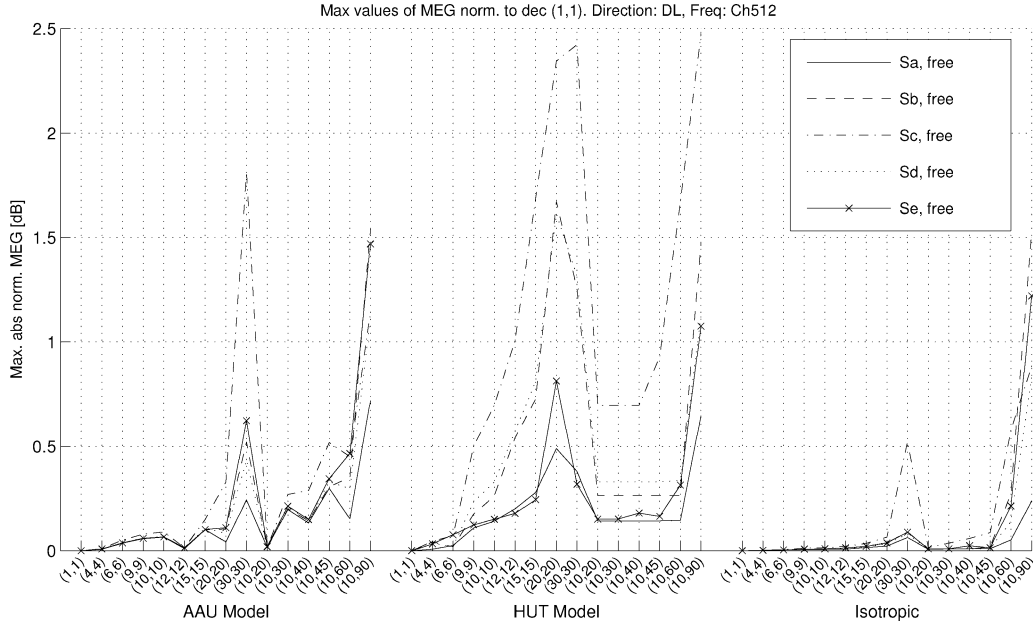
Fig. 7. MEG for simulated handsets versus sampling increment in θ and ϕ angle. The values are normalized to the MEG for a $1° \times 1°$ grid.

which is where most power exists for both the AAU and HUT models.

The simulation results indicate that a denser sampling is required than predicted by the theory given in [25]. One reason may be that the radiation patterns were not reconstructed using ideal basis functions but instead uses the samples directly in the approximation sum of the integrals, as shown in (2).

Based on the simulated results it was decided to use a sampling increment of $10°$ in both the azimuth and elevation angles of the radiation pattern measurements carried out in the anechoic room. This was deemed an acceptable compromise between measurement time and accuracy. For this sampling density the simulated radiation patterns result in a maximum absolute error of 0.1 dB for the AAU model while for the HUT model it is less than or equal to 0.3 dB for all antennas except Sc which results in a value of 0.7 dB. However, the standard deviation is maximum 0.2 dB in any case.

It is expected that a larger sampling interval, i.e., fewer measurements points and hence less time, are acceptable in practice for performance evaluations of most handsets. The rather dense sampling was deliberately chosen to allow an investigation of the error introduced in the MEG, when a coarser sampling is used during the measurements. The change in the MEG was investigated by decimation of the actually measured radiation patterns, i.e., using different values of p and q in (2). By using this procedure the radiation patterns are exactly as if the measurements were made with a larger sampling interval including all imperfections in the measurements. In this way it is taken into account that the averaging inherent in the MEG calculation may reduce the influence of imperfections in the measurements, such as reflections in the anechoic room, if enough samples are included.

Due to the physical shape of the handsets, where the length is larger than the width, it can be advantageous to use a denser sampling for the elevation angle than for the azimuth angle, as verified by the FDTD simulation results discussed above. Below

decimation is generally indicated using the notation $(p+r, q+s)$, in which case the samples are located at the angles $\theta_n = n \cdot p\Delta_\theta + r\Delta_\theta$ and $\phi_m = m \cdot q\Delta_\phi + s\Delta_\phi$, where $\Delta_\theta = \Delta_\phi = 10°$.

Fig. 8 shows example results of the normalized MEG given by (3) for handset C and E, where the endpoints of each vertical line are given by the minimum and maximum values of $\Gamma'_{p,q}(\lambda, \mu)$ obtained with the different handset orientations. In addition the mean value is shown as a point on the line.

From Fig. 8. it is noticed that the deviation results obtained with the isotropic, rect0, and rect6 models are similar, which is a general tendency for all handsets. As mentioned above, the non-zero part of the rectangular windows cover a large part of the sphere and therefore, similarly to the isotropic model, results in a summation of many samples, even if the decimation factor is high. Furthermore, in these models all samples are weighted equally (inside the window). This makes the models relatively insensitive to coarse sampling, as compared to the AAU and HUT models.

The results in Fig. 8 for the two handsets are clearly different for the AAU and HUT models, which may be due to the type of handsets. Both handset C and E are small, but handset E uses a large extractable dipole which is more directive than the internal antenna used by handset C. This explains the rather low error for handset C particularly for a decimation factor of 6 in both azimuth and elevation. For the remaining handsets the results are more equal, probably because of the similar sizes. When the phantom is included in the measurements the differences observed with handset C and E are less significant, most likely due to the large size of the phantom which makes the radiation more alike (by reflection and blocking).

As expected, for free space conditions the MEG error variation for the AAU model is generally lower for decimation factors $p = q = 2$ than for a factor of 3. However, this is not the case for the HUT model where the two sampling densities result in a similar variation, and in several cases the results for a factor of 2 are worse than those for a factor of 3. Although the HUT
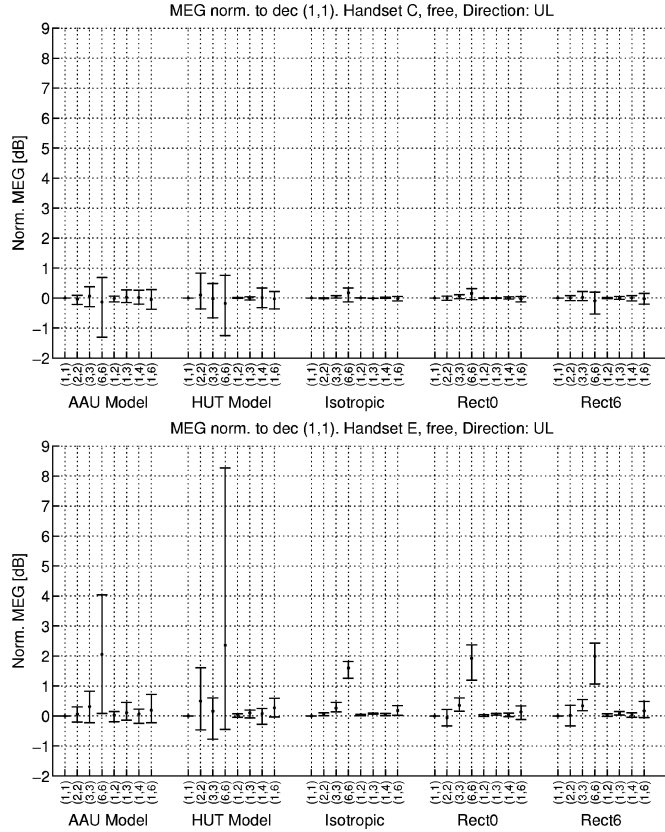
Fig. 8. MEG versus sample grid decimation for handset C (top) and handset E (bottom), Both in free space and for the UL. The values are normalized to the MEG for a $10° × 10°$ grid.

model is constant versus azimuth angle it is rather selective in the elevation angle, and it is therefore more sensitive towards where the samples are taken. The same remarks can be made concerning the phantom measurements, although the tendency is less pronounced.

Statistics computed from the combined data, i.e., the data originating from all handsets in both the UL and DL direction are pooled into a single data set, are given in Table IV for both the free space and the phantom case. For all the tested combinations of decimation factors $(p+r, q+s)$ and the different channel models, both the mean ("Mean") and standard deviation ("Std") of the normalized MEG (in dB), as well as the maximum absolute value ("Max Abs") have been computed.

From Table IV it is noticed that the errors obtained with the isotropic and rectangular models are similar, except that with the isotropic model the errors are usually slightly smaller. Furthermore, with a few exceptions the Iso, rect0, and rect6 models result in standard deviations and maximum absolute errors that are smaller than the corresponding values for the AAU and HUT models. Therefore, the following analysis focus on the latter two models.

Comparing the results obtained with and without the phantom, the standard deviations are roughly the same, except for the HUT model where the standard deviation increases when the phantom is included and a ϕ-angle decimation factor of 6 is used.

From Table IV it is noticed that for free space the error observed with the HUT model and the (2,2) decimation is larger than that obtained with the (3,3) decimation, with regards to the mean, standard deviation, and maximum absolute error. Unlike the case of (3,3) decimation, decimation with factors (2,2) means that no sample is used from $\theta = 90°$ which is important with the HUT model, since it is very selective in the elevation angle. This illustrates that not only the number of samples but also their locations on the sphere are important. The results for the offset sampling grids $(2 + 1, 2)$ and $(6 + 3, 6)$ support this. For the HUT model the $(2+1, 2)$ sampling grid reduces the standard deviation of the error from 0.7 to 0.3 dB obtained with the (2,2) grid. The influence is even larger on the (6,6) grid where the offset results in a change in the mean of 2.7 dB.

If all the environment models are considered it may be concluded from the above results that using a decimation of (1,2), corresponding to sampling in a $10° × 20°$ grid, leads to negligible errors. The maximum absolute change observed for this decimation is 0.4 dB, which should be compared to the MEG changes of the order 6–8 dB obtained in Section IV.

In case the HUT model is not applied, using decimation factors (2,2) is attractive since the maximum absolute MEG error observed in this case is 0.5 dB. Alternatively, decimation with factors (1,4) could be used, which showed a maximum absolute error of 0.6 dB. The latter grid is furthermore preferable for the HUT model, especially for free space. Comparing the results for the offset grids $(2 + 1, 2)$ and $(1, 4 + 2)$ with those for the (2,2) and (1,4) grids, sampling in a $10° × 40°$ grid seems slightly more insensitive to sampling location, as judged by the standard deviations.

For computing TRP and TIS sampling in a $10°$ by $40°$ grid or a $20°$ by $20°$ leads to a maximum error of 0.3 dB, which should be compared to the TRP/TIS differences of 2–3 dB observed among the handsets.

The results obtained from the measured data can be compared to the results based on the FDTD simulations presented in Section V. Also for the simulated data sampling in a $10° × 40°$ grid is significantly better for the HUT model than a $20° × 20°$ grid, with a reduction of the maximum absolute error from 2.3 to 0.7 dB and from 0.6 to 0.1 dB for the standard deviation, when all the antennas are considered as a whole. It is important to notice that no interpolation error is included in these results, as mentioned previously.

VI. MEASUREMENT FREQUENCY INFLUENCE ON MEG

In the following the differences in the MEG for three measurement frequencies are evaluated using the normalized MEG

$$\Gamma^*(f; \lambda, \mu) = \frac{\Gamma(f; \lambda, \mu)}{\Gamma(f_c; \lambda, \mu)} \quad (4)$$

where f_c is the frequency of the center GSM-1800 channel 698, i.e., 1842 MHz for the DL and 1747 MHz for the UL. The MEG value $\Gamma(f; \lambda, \mu)$ is computed as in (2) with the gain pattern $G_\psi(\cdot)$ measured at the frequency f and using rotation angles

TABLE IV
STATISTICS OF THE ERROR IN MEG OBTAINED WITH DECIMATED MEASUREMENTS. ALL STATISTICS ARE DERIVED FROM VALUES IN dB

	$(p+r, q+s)$	Free Space					Phantom				
		AAU	HUT	Iso	Rect0	Rect6	AAU	HUT	Iso	Rect0	Rect6
Mean	$(2,2)$	0.0	0.3	0.0	0.0	0.0	0.0	0.1	0.0	0.0	0.0
	$(2+1,2)$	0.0	−0.1	0.0	0.0	0.0	−0.1	−0.1	−0.1	−0.1	−0.1
	$(3,3)$	0.1	−0.1	0.0	0.1	0.1	−0.1	−0.1	−0.1	−0.1	−0.1
	$(6,6)$	1.1	1.2	0.9	1.1	1.1	0.2	1.2	0.4	0.2	0.0
	$(6+3,6)$	−1.6	−1.5	−1.0	−2.0	−1.9	−0.4	−0.1	−0.8	−0.3	−0.1
	$(1,2)$	0.0	0.0	0.0	0.0	0.0	0.0	0.0	0.0	0.0	0.0
	$(1,3)$	0.0	0.0	0.0	0.0	0.0	0.0	0.0	0.0	0.0	0.0
	$(1,4)$	0.0	0.0	0.0	0.0	0.0	0.0	0.0	0.0	0.0	0.0
	$(1,4+2)$	0.0	0.0	0.0	0.0	0.0	−0.1	−0.1	−0.1	−0.1	−0.1
	$(1,6)$	0.0	0.0	0.0	0.0	0.0	0.2	0.3	0.1	0.1	0.2
Std	$(2,2)$	0.1	0.7	0.0	0.1	0.2	0.1	0.5	0.1	0.2	0.2
	$(2+1,2)$	0.1	0.3	0.0	0.1	0.1	0.1	0.3	0.1	0.2	0.2
	$(3,3)$	0.3	0.5	0.2	0.2	0.2	0.2	0.5	0.1	0.1	0.1
	$(6,6)$	1.0	2.0	0.4	0.6	0.7	1.0	2.9	0.4	0.6	0.7
	$(6+3,6)$	1.4	1.6	0.6	1.6	2.0	0.8	1.0	0.6	0.7	0.8
	$(1,2)$	0.0	0.0	0.0	0.0	0.0	0.1	0.1	0.0	0.0	0.0
	$(1,3)$	0.1	0.1	0.0	0.0	0.0	0.1	0.2	0.0	0.0	0.0
	$(1,4)$	0.1	0.1	0.0	0.0	0.0	0.1	0.2	0.1	0.1	0.1
	$(1,4+2)$	0.1	0.1	0.0	0.0	0.0	0.2	0.2	0.1	0.1	0.1
	$(1,6)$	0.2	0.2	0.1	0.1	0.1	0.4	0.7	0.2	0.2	0.3
Max Abs	$(2,2)$	0.3	2.1	0.1	0.3	0.4	0.5	1.2	0.2	0.5	0.7
	$(2+1,2)$	0.3	0.9	0.1	0.3	0.3	0.6	1.0	0.3	0.4	0.5
	$(3,3)$	1.0	1.8	0.5	0.6	0.8	0.8	1.6	0.3	0.4	0.3
	$(6,6)$	4.0	8.3	1.8	2.4	2.4	3.2	6.5	1.4	1.9	2.1
	$(6+3,6)$	5.2	5.7	2.6	6.5	7.5	2.4	3.1	2.1	1.8	2.0
	$(1,2)$	0.3	0.2	0.1	0.0	0.1	0.4	0.3	0.1	0.1	0.1
	$(1,3)$	0.5	0.3	0.1	0.1	0.2	0.7	0.8	0.1	0.1	0.2
	$(1,4)$	0.4	0.5	0.1	0.1	0.2	0.6	1.0	0.2	0.4	0.5
	$(1,4+2)$	0.6	0.5	0.1	0.1	0.2	1.3	1.2	0.3	0.3	0.4
	$(1,6)$	1.1	1.0	0.4	0.3	0.6	1.9	2.7	0.6	0.9	1.2

λ and μ. Based on the results presented in Section V, all the investigations discussed in this section are carried out using measurements with a sampling of $10°$ in the elevation angle and $20°$ in the azimuth angle.

Fig. 9 shows an example of the results obtained with handset F in the UL. In the plot the minimum and maximum values of the $\Gamma^*(\cdot)$ values obtained at different handset orientations defines the endpoints of vertical lines. A line is shown for each combination of environment model and the two sets of values, obtained at the lowest and highest frequencies, respectively. The lowest frequency is 1805 and 1710 MHz for the DL and UL, respectively, while the highest frequency is 1880 and 1785 MHz for the DL and UL, respectively.

From Fig. 9 it is noted that for channel 512 all of the values are negative with a mean value of about −1 dB. For channel 885 most values are positive with mean values of approximately 0.25 dB. It is noticed that the results obtained with the Isotropic, Rect0, and Rect6 are again very similar, and this is a general tendency for all the handsets. In the following only results for the AAU, HUT, and Isotropic models are discussed.

Table V shows the mean, standard deviation, and maximum absolute values of the $\Gamma^*(\cdot)$ obtained with all the handsets in both UL and DL for the phantom measurements. For brevity the similar table for the free space results is omitted.
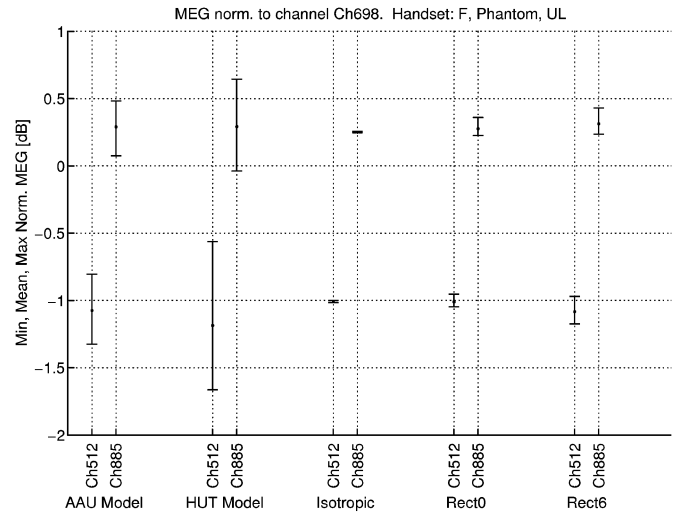

Fig. 9. Difference in MEG due to frequency for handset F in the UL and including the phantom.

Table V shows that all the mean values are in the range −2.6 to 2.0 dB for the phantom case, while the range for the free space measurements is −2 to 1.3 dB. Thus, there is a significant variation in power over the frequency band. From the tables it

TABLE V
STATISTICS OF THE DIFFERENCE IN MEG OBTAINED AT DIFFERENT CHANNELS FOR THE PHANTOM MEASUREMENTS. ALL STATISTICS ARE DERIVED FROM VALUES IN dB

		Ch512–Ch698			Ch885–Ch698		
	Handset	AAU	HUT	Iso	AAU	HUT	Iso
Mean, DL	A	−0.4	−0.4	−0.4	−1.6	−2.6	−0.9
	B	0.4	0.3	0.5	0.9	2.0	0.1
	C	0.6	0.8	0.4	−1.0	−1.0	−0.9
	E	−0.9	−0.9	−0.8	−0.8	−0.6	−0.8
	F	−0.5	−0.5	−0.6	−0.5	−0.5	−0.5
Mean, UL	A	0.0	−0.1	0.1	−0.1	−1.2	0.8
	B	−0.7	−0.7	−0.7	−0.3	0.9	−1.2
	C	−0.7	−0.5	−0.8	−1.1	−1.1	−1.1
	E	−0.5	−0.7	−0.4	−0.5	−0.5	−0.6
	F	−1.1	−1.2	−1.0	0.3	0.3	0.3
Std, DL	A	0.1	0.2	0.0	0.6	0.8	0.0
	B	0.2	0.4	0.0	0.7	1.0	0.0
	C	0.1	0.1	0.0	0.1	0.2	0.0
	E	0.1	0.2	0.0	0.1	0.3	0.0
	F	0.1	0.2	0.0	0.1	0.2	0.0
Std, UL	A	0.1	0.2	0.0	0.7	1.3	0.0
	B	0.1	0.3	0.0	0.9	1.6	0.0
	C	0.1	0.1	0.0	0.1	0.2	0.0
	E	0.2	0.3	0.0	0.1	0.2	0.0
	F	0.1	0.3	0.0	0.1	0.2	0.0
MaxAbs, DL	A	0.6	0.8	0.4	2.6	4.1	0.9
	B	0.7	0.9	0.5	2.5	3.8	0.1
	C	0.8	1.1	0.4	1.2	1.3	0.9
	E	1.2	1.2	0.9	1.1	1.0	0.8
	F	0.7	0.7	0.6	0.7	0.7	0.5
MaxAbs, UL	A	0.2	0.3	0.1	1.7	3.3	0.8
	B	1.0	1.3	0.7	2.1	3.7	1.2
	C	0.9	0.6	0.8	1.3	1.5	1.1
	E	1.0	1.2	0.4	0.8	0.7	0.6
	F	1.3	1.7	1.0	0.5	0.6	0.3

furthermore appears difficult to predict the mean difference at one end of the band if the mean difference is known at the other band edge.

With a few exceptions, the mean values obtained with the three different environments are usually within a few tenths of a dB, but corresponding mean values for the UL and DL are often not similar. The maximum absolute ("Max Abs") values shows that computing the MEG from a measurement made at the center channel may result in an error of up to 4.1 dB at the band edges for the phantom, where the value for the free space is 3.0 dB.

VII. REDUCED SAMPLING IN FREQUENCY

The results of Section VI show that measurements at the center channel cannot be used at the band edges without significant errors. Hence, a number of channels have to be measured for accurate results. However, not all of the measurements on the different channels need to include all spherical measurement points, as shown below.

Define the total antenna efficiency at the frequency f as

$$\gamma(f) = \oint_S G_\theta(\Omega, f) + G_\phi(\Omega, f) d\Omega. \tag{5}$$

Using this definition, the frequency dependent MEG in (1) may be written as

$$\Gamma(f) = \gamma(f)\hat{\Gamma}(f) \tag{6}$$

where $\hat{\Gamma}(f)$ is the MEG obtained from the radiation patterns normalized to a total antenna efficiency of 100%, i.e., $\hat{\Gamma}(f)$ is obtained by substituting the normalized antenna gain patterns given by $G'_\psi(\Omega, f) = G_\psi(\Omega, f)/\gamma(f)$ in (1). If it can be shown that $\hat{\Gamma}(f_1) \simeq \hat{\Gamma}(f_2)$ for any f_1, f_2 within the band of interest, then the full spherical radiation pattern of the antenna only has to be measured at one frequency. The MEG at other frequencies may be obtained by a simple scaling, as indicated by (6). Obviously, this is only an advantage if $\gamma(f)$ can be estimated from a fewer number of samples than used in the integration for $\hat{\Gamma}(f)$.

The expression for $\gamma(f)$ in (5) is almost the same as that for $\Gamma(f)$ in the isotropic case and the results in Section V concerning sampling density can be used to assess how well $\gamma(f)$ can be estimated from few samples. For the isotropic environment it is easily shown that

$$\frac{\Gamma_{p,q}}{\Gamma_{1,1}} = \frac{\gamma_{p,q}}{\gamma_{1,1}} \cdot \frac{\sum_{n=0}^{N-1} \sin(\theta_n)}{p \sum_{n=0}^{\frac{N-1}{p}} \sin(\theta_{p \cdot n})} \tag{7}$$

where the approximated value of $\gamma(f)$ is given by

$$\gamma_{p,q} = pq\Delta_\theta\Delta_\phi \sum_{n=0}^{\frac{N-1}{p}} \sum_{m=0}^{\frac{M}{q}-1} [G_\theta(\theta_{p \cdot n}, \phi_{q \cdot m}) \\ + G_\phi(\theta_{p \cdot n}, \phi_{q \cdot m})] \sin(\theta_{p \cdot n}).$$

Similarly to the notation used previously, (p, q) are the decimation factors used on the original measurements, and the ratio $\gamma_{p,q}/\gamma_{1,1}$ is a measure of how close the γ value computed using decimated measurements is to the value $\gamma_{1,1}$ obtained using the non-decimated measurements.

Equation (7) shows that statistics about $\gamma_{p,q}/\gamma_{1,1}$ can be obtained from the results presented in Table IV (the isotropic environment). Depending on the value of p, the following figures have to be subtracted from the mean values:

p	1	2	3	6
α[dB]	0	0.03	0.09	0.41

where α is the second product term of (7) involving the ratio of two summations, expressed in decibels. The standard deviation values in Table IV need no correction. From these numbers it is clear that $\gamma(f)$ can be estimated with small errors, even with rather large sampling intervals. The maximum absolute mean values are 0.2 and 1.4 dB for $p = 3$ and $p = 6$, respectively, considering both the free space and phantom measurements. The standard deviations are 0.2 dB for $p = 3$ and 0.6 dB for $p = 6$. Note that due to the non-linear nature of the "Max Abs" operation, these numbers cannot be obtained by simple subtraction.

Regarding the variation in $\hat{\Gamma}(\cdot)$ versus frequency, it is easily shown that

$$\frac{\hat{\Gamma}(f; \lambda, \mu)}{\hat{\Gamma}(f_c; \lambda, \mu)} = \frac{\Gamma^*(f; \lambda, \mu)}{\Gamma^*_{\text{iso}}(f; \lambda, \mu)}$$

where $\Gamma^*_{\text{iso}}(\cdot)$ is the value of (4) computed for the isotropic environment. Hence, the variation over frequency of the normalized MEG $\hat{\Gamma}(\cdot)$ for the non-isotropic environments may be obtained by normalizing $\Gamma^*(\cdot)$ with the value from the isotropic case. From the example in Fig. 9 it is evident that this may lead to a reduction of the maximum error in the MEG.

As noted in Section VI, the mean values of $\Gamma^*(\cdot)$ obtained with the different models are often approximately the same. If the values indeed are identical then the mean error in the normalized MEG, $\hat{\Gamma}(\cdot)$, is zero and the standard deviations are given in Table V in the "Std" rows. In practice, the mean value of $\hat{\Gamma}(\cdot)$ is not zero in all cases but in most cases the magnitude is reduced, so that only 11 mean values out of a total 40 are larger than 0.2 dB. Most of the values exceeding 0.2 dB are for Handset A and B on channel 885. This can be compared to the values obtained with the non-normalized measurements, where 37 of the mean values exceed 0.2 dB.

Hence, the error due to frequency variation can be reduced even when taking into account that the estimation of $\gamma(f)$ is not perfect, as assumed in the last paragraph. Choosing to estimate $\gamma(f)$ from a (1,4) grid leads to a mean and maximum error of 0.0 dB and 0.1 dB (see Table IV), respectively and hence will not offset the obtained reduction in mean error.

The statistics of the frequency variation of $\hat{\Gamma}$ have been investigated using a table similar to Table V, omitted here for brevity. The standard deviation values of $\hat{\Gamma}(\cdot)$ are identical to those given in Table V and usually below 0.4 dB for both the free space and phantom measurements. Exceptions to this are handset A and B for channel 885 using the phantom with values 0.6–1.6 dB. For the free space measurements handset E is the only example where the standard deviation exceeds 0.4 dB with values 0.5–1.0 dB.

The numbers given above may be compared with what was obtained from a similar investigation using the simulated antennas described in Section V. Here the maximum standard deviation was 0.4 dB for the HUT model and 0.2 dB for the AAU model, considering all five antennas in free space.

VIII. CONCLUSION

For the environment models based on measurements, a variation in the MEG of 5–8 dB for different orientations was found when the handset is next to the phantom. In addition, some significant differences in the MEG variation have been observed for the two models based on measurements. The models not based on measurements do not result in as much variation in the MEG. In particular, the isotropic environment resulting in MEG values corresponding to TRP and TIS, has no variation by definition. A slightly more realistic rectangular window model having an XPD of 6 dB resulted in a variation up to about 3 dB.

As expected, the MEG values computed using models which are isotropic, or essentially isotropic, were found to be influenced less by a reduced sampling density than the MEG values obtained with the two measurement based, non-isotropic models of the power distribution. Considering all the environment models, a sampling density of $10° \times 20°$ (elevation angle $\times$ azimuth angle) resulted in a maximum error of 0.4 dB and a standard deviation of 0.1 dB. If the HUT model is not applied, a sampling density of $20° \times 20°$ may be attractive, in which case the maximum error observed was 0.5 dB and the standard deviation was 0.2 dB. The results obtained with the isotropic environment showed that total power results (TRP and TIS) can be obtained within a maximum error of 0.5 dB if a $30° \times 30°$ sampling grid is used.

The frequency variation of the MEG was investigated using measurements made at the center channel and at the two edge channels of the GSM-1800 band. The change in MEG at the band edges relative to the center channel, computed as the mean over all the handset orientations, were in the range -2.6 up to 2.0 dB for the phantom case. While the value depends on the link direction and the handset, the results for the different environment models are usually within a few tenths of a dB.

With the purpose of reducing the total number of measurements it was proposed to divide the MEG into a frequency dependent total power term and a, ideally, frequency independent normalized MEG term. It was shown in this work that the frequency dependent total power can be estimated within a fraction of a dB by using only a small subset of the full spherical radiation pattern. Using the estimated total power the frequency dependence of the MEG cannot be removed completely, but the mean difference is usually significantly reduced.

REFERENCES

[1] W. C. Jakes, Ed., *Microwave Mobile Communications*. New York: IEEE Press, 1974.

[2] J. B. Andersen and F. Hansen, "Antennas for VHF/UHF personal radio: a theoretical and experimental study of characteristics and performance," *IEEE Trans. Veh. Technol.*, vol. 26, no. 4, pp. 349–357, Nov. 1977.

[3] M. Murase, Y. Tanaka, and H. Arai, "Propagation and antenna measurements using antenna switching and random field measurements," *IEEE Trans. Veh. Technol.*, vol. 43, no. 3, pp. 537–541, Aug. 1994.

[4] G. F. Pedersen, J. Ø. Nielsen, K. Olesen, and I. Z. Kovacs, "Measured variation in performance of handheld antennas for a large number of test persons," Proc. 48th Vehicular Technology Conf., VTC '98 IEEE, May 1998, pp. 505–509.

[5] W. A. T. Kotterman, G. F. Pedersen, and P. Eggers, "Cable-less measurement set-up for wireless handheld terminals," in *Proc. 12th Int. Symp. Personal, Indoor and Mobile Radio Communications (PIMRC 2001)*, Sep. 2001, pp. B112–B116.

[6] J. Ø. Nielsen, G. F. Pedersen, and C. Solis, "In-network evaluation of mobile handset performance," in *Proc. IEEE Vehicular Technology Conf. (VTC'2000 Fall)*, Sep. 2000.

[7] J. Ø. Nielsen and G. F. Pedersen, "In-network evaluation of body carried mobile terminal performance," in *Proc. 12th Int. Symp. Personal, Indoor and Mobile Radio Communications (PIMRC 2001)*, Sep. 2001, vol. 1, pp. D-109–D-113.

[8] L. M. Correia, Ed., *Wireless Flexible Personalised Communications. COST 259: European Co-Operation in Mobile Radio Research*. New York: Wiley, 2001.

[9] N. Ohnishi, K. Sasaki, and H. Arai, "Field simulator for testing handset under multi-path propagation environments," in *Antennas and Propagation Society International Symp., 1997 Digest*, 1997, vol. 4, pp. 2584–2587.

[10] K. Rosengren, P.-S. Kildal, J. Carlsson, and O. Lundén, "A new method to measure radiation efficiency of terminal antennas," in *Proc. IEEE-APS Conf. Antennas and Propagation for Wireless Communications*, 2000, pp. 5–8.

[11] J. Krogerus, K. Kiesi, and V. Santomaa, "Evaluation of three methods for measuring total radiated power of handset antennas," in *Proc. 18th IEEE Instrumentation and Measurement Technology Conf.*, 2001, vol. 2, pp. 1005–1010.

[12] T. Taga, "Analysis for mean effective gain of mobile antennas in land mobile radio environments," *IEEE Trans. Veh. Technol.*, vol. 39, no. 2, pp. 117–131, May 1990.

[13] J. Toftgard, S. N. Hornsleth, and J. B. Andersen, "Effects on portable antennas of the presence of a person," *IEEE Trans. Antennas Propag.*, vol. 41, no. 6, pp. 739–746, 1993.

[14] G. F. Pedersen, J. B. Andersen, and S. Skjærris, "Integrated handset antenna with low absorption and handset antenna diversity," in *Inst. Elect. Eng. Colloquium on Design of Mobile Handset Antennas for Optimal Performance in the Presence of Biological Tissue (Digest 1997/022)*, 1997, pp. 4/1–4/5.

[15] M. G. Douglas, M. Okoniewski, and M. A. Stuchly, "A planar diversity antenna for handheld PCS devices," *IEEE Trans. Veh. Technol.*, vol. 47, no. 3, pp. 747–754, Aug. 1998.

[16] G. F. Pedersen, M. Tartiere, and M. B. Knudsen, "Radiation efficiency of handheld phones," 50th Vehicular Technology Conf., VTC'2000 IEEE, May 2000.

[17] K. Boyle, "Mobile phone antenna performance in the presence of people and phantoms," in *Proc. Inst. Elect. Eng. Antennas and Propagation Professional Network Technical Seminar: Antenna Measurement and SAR*, May 2002, pp. 8/1–8/4.

[18] K. Sulonen, K. Kalliola, and P. Vainikainen, "Comparison of evaluation methods for handset antennas," Millenium Conf. Antennas & Propagation, AP2000 European Space Agency. ESA Publications Division, 2000.

[19] K. Kalliola, K. Sulonen, H. Laitinen, O. Kivekäs, J. Krogerus, and P. Vainikainen, "Angular power distribution and mean effective gain of mobile antenna in different propagation environments," *IEEE Trans. Veh. Technol.*, vol. 51, no. 5, pp. 823–838, Sep. 2002.

[20] M. B. Knudsen and G. F. Pedersen, "Spherical outdoor to indoor power spectrum model at the mobile terminal," *IEEE J. Select. Areas Communicat.*, vol. 20, no. 6, pp. 1156–1169, Aug. 2002.

[21] Cellular Telecommunications & Internet Association (CTIA), CTIA Test Plan for Mobile Station Over the Air Performance, Revision 2.0 CTIA, Mar. 2003 [Online]. Available: http://www.ctia.org, Tech. Rep.

[22] European Telecommunications Standards Institute (ETSI), Global System for Mobile Communications (GSM) Specifications GSM 05.08.

[23] Schmid & Partner, http://www.speag.com/. Generic torso phantom, v.3.6.

[24] J. Graffin, N. Rots, and G. F. Pedersen, "Radiations phantom for handheld phones," in *Proc. 52nd Vehicular Technology Conf., Fall VTC 2000*, 2000, vol. 2, pp. 853–866.

[25] O. M. Bucci and G. Franceschetti, "On the spatial bandwidth of scattered fields," *IEEE Trans. Antennas Propag.*, vol. AP-35, no. 12, pp. 1445–1455, Dec. 1987.

[26] O. M. Bucci, C. Gennarelli, and C. Savarese, "Optimal interpolation of radiated fields over a sphere," *IEEE Trans. Antennas and Propag.*, vol. 39, no. 11, pp. 1633–1643, Nov. 1991.

Jesper Ødum Nielsen received the master's degree in electronics engineering in 1994 and the Ph.D. degree in 1997, both from Aalborg University, Aalborg, Denmark.

He is currently employed at the Department of Communication Technology at Aalborg University where his main areas of interests are experimental investigation of the mobile radio channel and the influence on the channel by mobile handset users. He has been involved in channel sounding and modeling, as well as measurements using the live GSM network. In addition he has been working with handset performance evaluation based on spherical measurements of handset radiation patterns and power distribution in the mobile environment. He is currently involved in MIMO channel sounding and modeling.

Gert Frølund Pedersen was born in 1965. He received the B.Sc.E.E. degree (with honors) in electrical engineering from the College of Technology, Dublin, Ireland, and the M.Sc.E.E. and Ph.D. degrees from Aalborg University, Aalborg, Denmark, in 1993 and 2003, respectively.

Since 1993, he has been employed by Aalborg University where he is currently working as a Professor with the Antenna & Propagation Group. His research has focused on radio communication for mobile terminals including small antennas, antenna-systems, propagation and biological effects. He has also worked as Consultant for developments of antennas for mobile terminals including the first internal antenna for mobile phones in 1994 with very low SAR, the first internal triple-band antenna in 1998 with low SAR, and high efficiency and various antenna diversity systems rated as the most efficient on the market. Recently, he has been involved in establishing a method to measure the communication performance for mobile terminals that can be used as a basis for a 3G standard where measurements also including the antenna will be needed. Furthermore, he is involved in small terminals for 4G including several antennas (MIMO systems) and ultrawideband antennas to enhance the data communication.